Australian Earthquake Engineering Society
2022 National Conference, 24-25 November 2022
Mount Macedon, Victoria, Australia

Paleoseismological study of a fault in Kalimantan, Indonesia – Challenges in a remote and humid environment

Dee Ninis[1], Astyka Pamumpuni[2], Naomi Maria Neysa Prayacita[2]

1. Seismology Research Centre, 141 Palmer Street, Richmond, Victoria, Australia

2. LAPI ITB, Jalan Sumur Bandung No. 5, Bandung, West Java, Indonesia

Abstract

Paleoseismological fault investigations in regions of slow tectonic deformation with humid climates are challenging due to the ease with which evidence of surface deformation is destroyed. We undertook a paleoseismological investigation of a fault in such a region - in Kalimantan, Indonesia. Our study employed elevation data to delineate a ~80 km-long fault, capable of hosting an earthquake of ~M_{max}7.1. Resistivity surveying identified possible sub-surface fault planes, however trenching at two sites exposed un-faulted alluvial deposits; samples collected from these yielded ages of between 136-281 cal BP at one site and 137-834 cal BP from the second site, suggesting no ground-rupturing earthquake on the fault in at least the last ~834 years. Because of the obvious surface expression of the fault in elevation imagery, we nonetheless suspect this structure is active, albeit with a low slip rate. Based on previously identified active faults in Kalimantan with similar morphological expressions, we infer a slip rate for this fault of 0.3-0.5 mm/yr.

Keywords: paleoseismology; active fault; radiocarbon dating; seismic hazard; Indonesia.

1 Introduction & Background

The paleoseismic characterisation of low slip rate faults in humid climate regions is difficult due to the long recurrence intervals between ground-rupturing earthquakes, in combination with the high erosion and deposition rates which quickly and easily destroy or bury evidence of previous tectonic surface deformation. Unlike other regions of Indonesia, Kalimantan – on the island of Borneo – typically experiences relatively infrequent moderate (>M5.0) to major (M>7.0) earthquakes (Figure 1). Some of the largest earthquakes to occur in this region include the 1923 M6.8 to the north of Mangkalihat Peninsula, the 1995 M6.1 off the coast of North Kalimantan Province, and the 2015 M6.1 in north Tarakan (PuSGeN, 2017). Based on the current understanding of neotectonic structures in Indonesia (PuSGeN, 2017), only two active faults have been identified in the northern part of Kalimantan – the Tarakan and Mangkalihat faults – (Figure 1); these are inferred to be the source of the aforementioned earthquakes.

In this investigation, we delineate the extent of a potentially active fault from remote sensing data and employ field investigations – namely the acquisition of resistivity data, paleoseismological trenching and radiocarbon dating – to determine prior ground-rupture

earthquake activity on this structure. This fault study was undertaken as part of a site-specific Seismic Hazard Analysis (SHA) in a remote and highly vegetated region of North Kalimantan. Lead by the Seismology Research Centre (SRC), the originally planned field investigations were hampered by the COVID-19 pandemic and associated travel restrictions, and were eventually undertaken by local experts on behalf of, and in collaboration with, the SRC. The exact location of the site remains 'commercial in confidence' on request of the client, but we here present the geological methodology and findings for characterising this fault in SHAs.

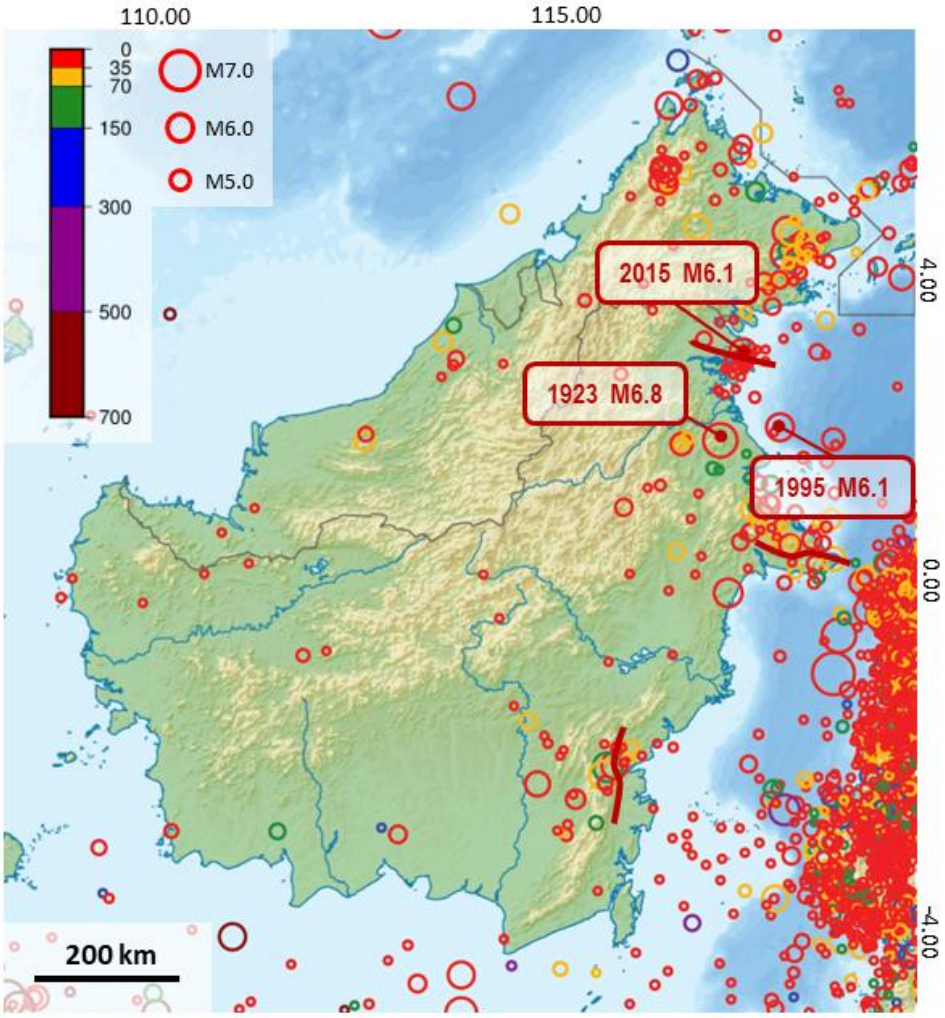

Figure 1. Kalimantan, Indonesia, on the island of Borneo, showing earthquakes plotted by depth, and known active faults (red lines) (PuSGeN, 2017).

Previous geological mapping (Heryanto et al., 1995) first identified the surface expression of this north-northwest striking fault, which, about mid-way along the fault and towards its northern extent, splays into two fault strands of similar orientation. Along the fault, Jurassic ultramafics and early Cretaceous schists are exposed, while the surrounding geology consists predominately of Late Cretaceous to early Paleocene sandstone to the west of the structure, and younger mid-Eocene sandstones to the east. The northwest orientation of the present-day crustal stress across this region (Tingay et al., 2010) suggest that in the current tectonic setting, this fault would accommodate left-lateral strike-slip rupture.

2 Methods

In this investigation, we first used Indonesia's National Seamless Digital Elevation Model (DEMNAS) (DEMNAS, n.d.) as well as lidar-derived elevation data and aerial photomosaic to delineate the extent of the fault. DEMNAS data is open access, downloadable data with 8 m horizontal resolution, while the lidar-dervied elevation data had a lateral resolution of 1 m. Fault traces delineated from this remote sensing data were then compared with regional geological maps (Heryanto et al., 1995) as well as field observations to confirm the fault location.

Reconnaissance field observations were undertaken with the objective of investigating the general geology (type and age of the lithology) and geomorphology of sites and, therefore, their suitability for active fault studies. Also of importance in this remote region of Kalimantan was information regarding the accessibility of each site for our more detailed field investigations.

Electrical resistivity survey profiles were undertaken across the fault to image subsurface geological structures, and to thereby aid in identifying the location of the near-surface fault plane in order to select suitable places for fault trenching. Importantly, for the site to be suitable for trenching, deposits needed to be young enough to provide evidence for recent ground rupture, so we focused on sites of late Quaternary deposits such as alluvial fans and fluvial terraces. Two sites were chosen – one on each of the fault strands at the southernmost extent of the fault. Finally, sediment samples were collected for radiocarbon age-dating to provide information on the timing of ground-rupturing earthquakes on the fault.

3 Results & Discussion

The analysis of elevation and aerial photomosaic data delineated a ~80 km-long fault, which we call the 'East Main Fault', with a north-western fault strand which we hereby refer to as the 'West Main Fault' - at ~41 km in length (Figure 2). Based on fault length and using Wells & Coppersmith (1994) we can infer a maximum magnitude for this fault of M_{max}6.9-7.1.

Field reconnaissance observations were conducted along both faults at seven locations in total. Based on these observations, the most suitable locations for further investigations of the West Main Fault was Area 1 (Figure 3, Figure 4); other areas along this fault were found to be devoid of young deposits and, therefore, active morphological evidence, or otherwise man-modified. Area 1 was investigated further to locate geomorphological evidence of the fault and to determine a suitable location for resistivity surveying. Access to Area 1 was only by long boat via the main river. The most suitable site chosen for East Main Fault was Area 2 (Figure 3, Figure 5). Area 2 has flat morphology, sandy alluvial deposits, less dense vegetation, access from a nearby village, and is along strike and across the river from where the fault observed in bedrock. Area 2 was therefore favoured for a paleoseismological investigation.

Two resistivity surveys were conducted across the West Main Fault in Area 1, and three were conducted on the East Main Fault in Area 2. All five resistivity survey lines were located on Quaternary sediment and crossed interpreted fault lines. Area 1 resistivity survey results (Figure 4) show a low resistivity anomaly in the cliff where the contact between bed rock and alluvial deposits was located. Low resistivity in Area 1 also correlated with the fault line interpreted from lidar and aerial photomosaic. Area 1 was therefore favoured for fault trenching. Resistivity results of Area 2 show a low anomaly in two of three lines (Figure 5). A low resistivity zone in Area 2 did not continue to the surface and appeared wider with depth. This may be due to a shallow water table in the area. The two low resistivity anomalies in Area 2 correlated with the fault location interpretated from lidar and aerial photomosaic.

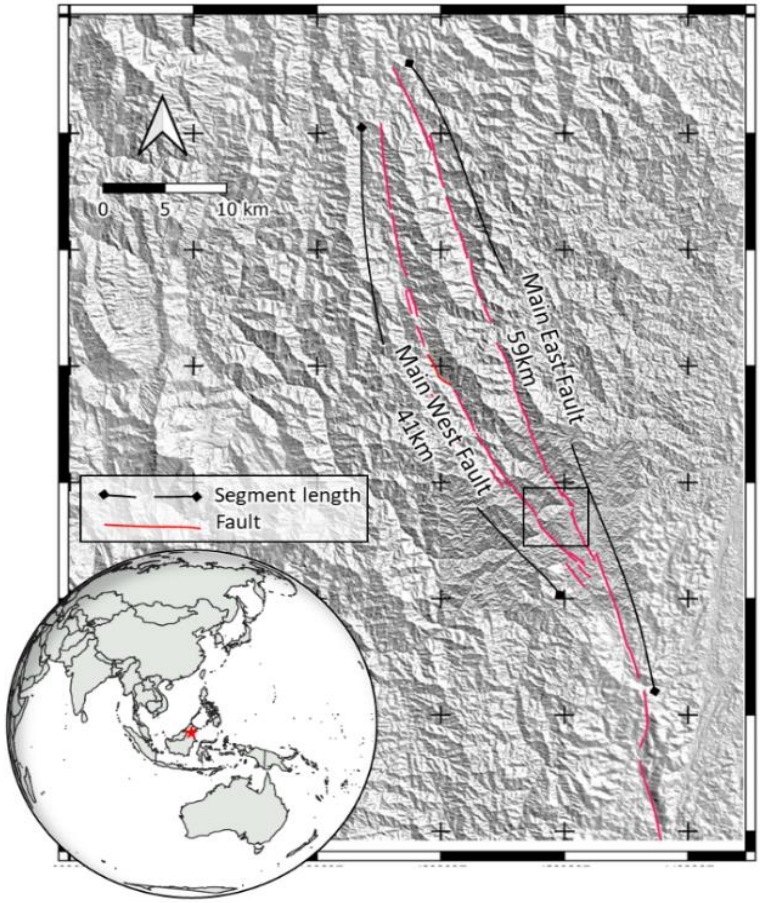

Figure 2: Paleoseismological study location and fault trace delineated from elevation data.

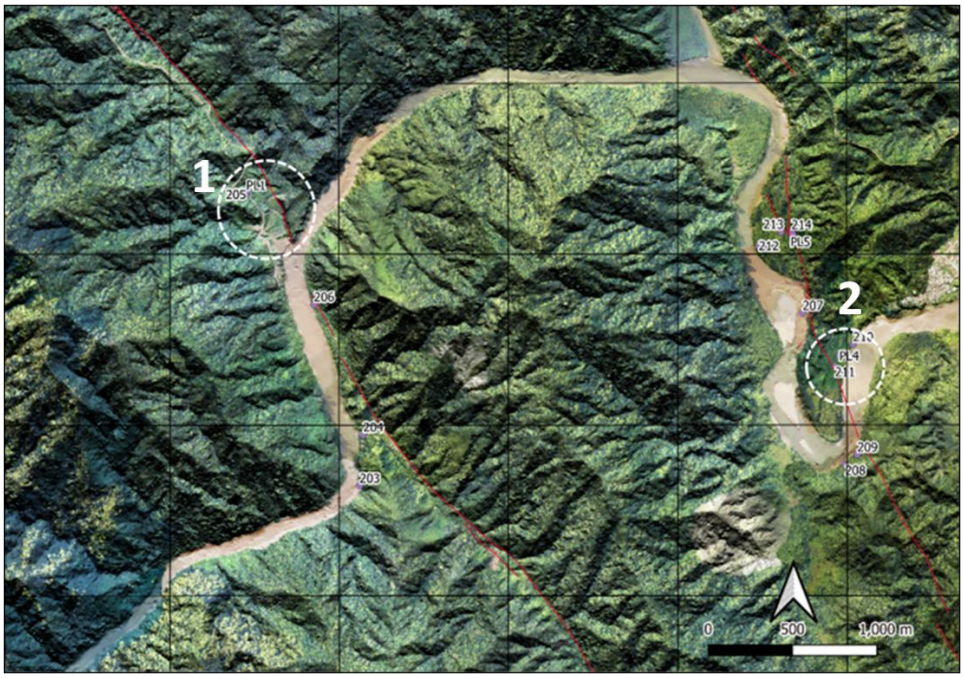

Figure 3. Area 1 and Area 2 field sites on West Main Fault and East Main Fault, respectively, as seen in photomosaic image.

Trenching was conducted in Areas 1 and 2, where the low resistivity anomaly corresponded to the lidar-interpreted fault location. Trenching in Area 1 was performed using manual digging and showed no evidence of ground rupture activity (Figure 4). Three samples from Area 1 taken from an alluvial sand deposit were sent for radiocarbon dating. Two samples show good confidence results, while one was inconsistent with the other two ages. The calibrated radiocarbon age of three samples in Area 1 are 281-170 cal BP, 225-136 cal BP, and 5909-5746 cal BP (Table 1). Trenching in Area 2 encountered a shallow water table and wall stability problems (Figure 5). The results show no evidence of ground rupture activity. Two samples from the trench location and two from the nearby riverbank were collected and sent for radiocarbon dating. Calibrated radiocarbon dating ages were all consistent, ranging from 224-137 cal BP to 834-732 cal BP (Table 1). All samples from the two trench locations showed very young sediment, with the oldest at 834 cal BP. Since there is no evidence of fault activity found in either of the fault trenches excavated, we infer that the West Main Fault and the East Main Fault have not produced ground rupturing earthquakes at least in the last 834 years.

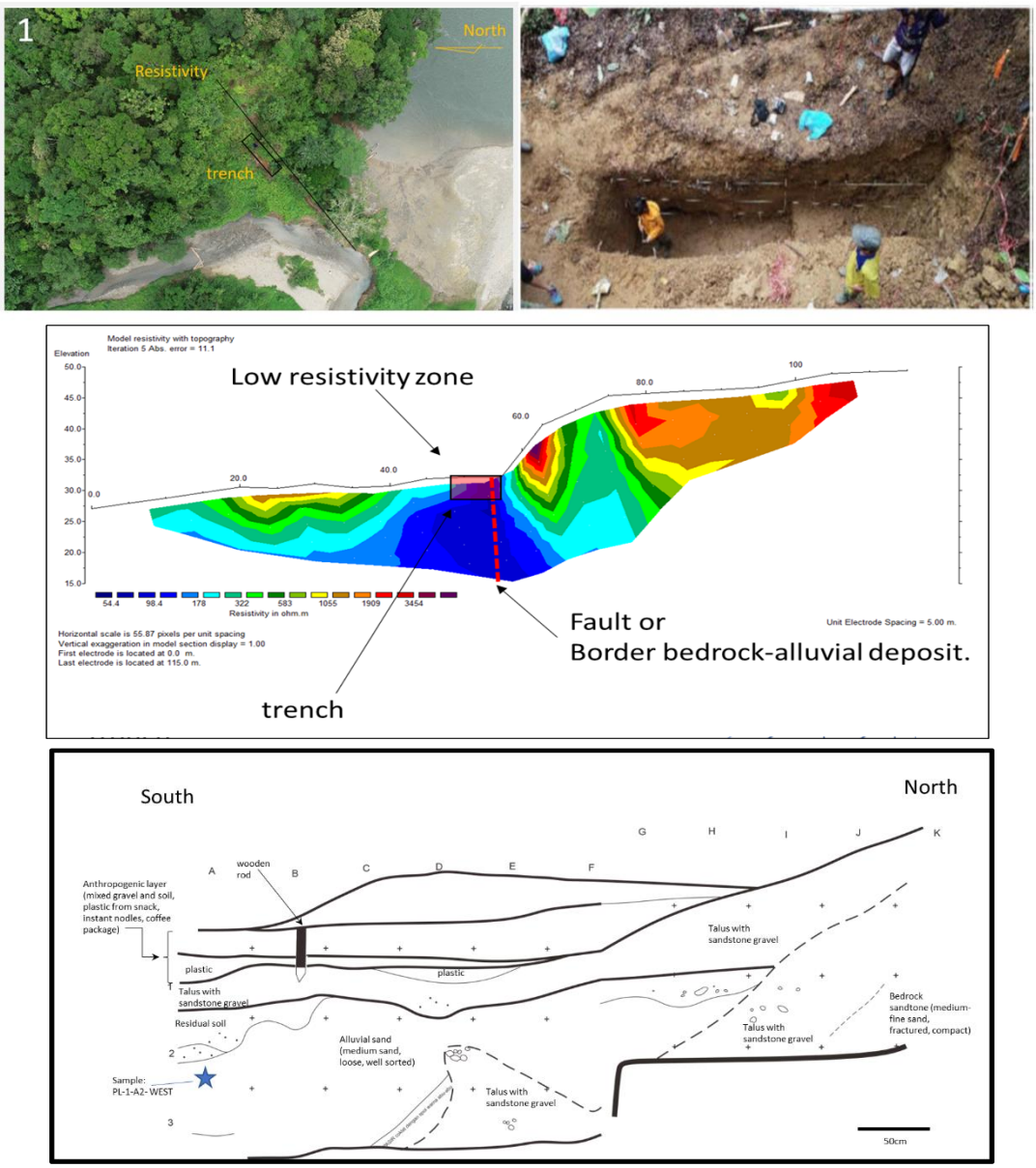

Figure 4. Area 1 West Main Fault: Top L - aerial photo showing location of resistivity profile and trench site; Top R – trench; Middle – resistivity profile; Bottom – trench log.

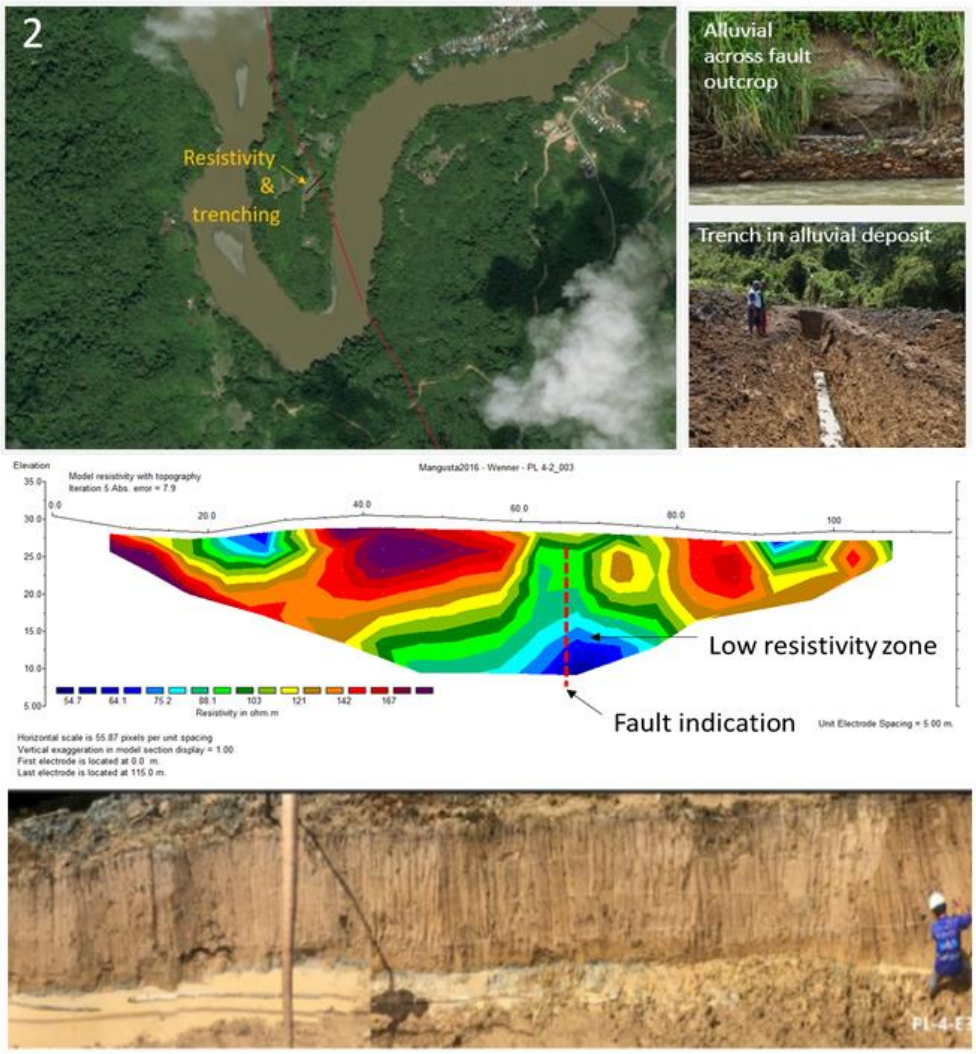

Figure 5. Area 2 East Main Fault: Top L - aerial photo showing location of resistivity profile and trench site; Top R – (upper) alluvial deposit along river bank, (lower) trench; Middle – resistivity profile; Bottom – trench wall.

Table 1. Radiocarbon sample description and ages

Sample	Material	Area	Conventional radiocarbon age ±30 BP	Calibrated radiocarbon age (95.4% probability) (cal AD)	(cal BP)	Probability (%)
PL-1-B3-EAST	organic sediment	PL-1-1	5080	3960-3797 cal BC	5909-5746	95.4
PL-1-ALT-A	woody material	PL-1-1	140	1669-1780	281-170	43.1
PL-1-A2-WEST	woody material	PL-1-1	180	1725-1814	225-136	53.4
PL-4-210-A2	woody material	PL-4	890	1116-1218	834-732	59.6
PL-4-210-A1	piece of charcoal	PL-4	190	1726-1813	224-137	55.1
PL-4-E3	woody material	PL-4	330	1477-1642	473-308	95.4
PL-4-2	woody material	PL-4	340	1470-1640	480-310	95.4

The results of our paleoseismological fault trench study and dating did not allow for a meaningful slip rate estimate to be made for the fault(s). Regardless, a fault slip rate was required for the SHA. Because of the obvious surface expression of the fault seen in lidar imagery and topographic data, we infer this structure may have ruptured within the Holocene, i.e., the last 11,000 years, and may therefore be active, albeit with a relatively low slip rate. Based on previously identified active faults in Kalimantan (c.f. PUSGEN, 2017) which are in the same tectonic setting, are similarly northwest-southeast oriented, and whose morphological expression appears similar - namely the Tarakan and Mangkalihat faults - we have assigned a slip rate to the fault of 0.3-0.5 mm/yr.

4 Conclusion

We undertook a paleoseismic investigation of a fault in a remote region in Kalimantan, Indonesia. Our study employed elevation data to delineate a ~80 km-long fault, capable of hosting an earthquake of ~Mmax7.1. Trenching at two sites exposed un-faulted alluvial deposits; samples collected from these suggest no ground-rupturing earthquake on the fault in at least the last ~834 years. However, the morphology of the fault is compatible with a fault which has been active during the Holocene (the last ~11,000 years) albeit with a low slip rate. Based on previously identified active faults in Kalimantan with similar morphological expressions, we infer a slip rate for this fault of 0.3-0.5 mm/yr.

Acknowledgements

The authors would like to thank Entura for permission to share the geological findings of this otherwise ‘commercial in confidence’ investigation.

References

DEMNAS. (n.d.). Retrieved February 22, 2022, from https://tanahair.indonesia.go.id/demnas/#/

Heryanto, R., Supriatna, S., & Abidin, H. Z. (1995). Geological Map of Malinau Sheet, Kalimantan. Geological Research and Development Center - Bureau of Mineral Resources.

Pusgen. (2017). Peta Sumber dan Bahaya Gempa Indonesia 2017. Pusat Penelitian dan Pengembangan Perumahan dan Permukiman Balitbang Kementrian PUPR.

Tingay, M., Morley, C., King, R., Hillis, R., Coblentz, D. and Hall, R., 2010. Present-day stress field of Southeast Asia. Tectonophysics, 482(1-4), pp.92-104.

Wells, D. L., & Coppersmith, K. J. (1994). New empirical relationships among magnitude, rupture length, rupture width, rupture area, and surface displacement. Bulletin - Seismological Society of America, 4, 974–1002.